COMPREHENSIVE RISK BASED METHODOLOGY AND TOOL FOR A QUANTITATIVE RESILIENCE ASSESSMENT OF DISTRIBUTION AND TRANSMISSION SYSTEMS

Andrea PITTO
Ricerca sul Sistema Energetico – Italy
andrea.pitto@rse-web.it

Claudio CARLINI
Ricerca sul Sistema Energetico – Italy
claudio.carlini@rse-web.it

Emanuele Ciapessoni
Ricerca sul Sistema Energetico – Italy
emanuele.ciapessoni@rse-web.it

Diego CIRIO
Ricerca sul Sistema Energetico – Italy
diego.cirio@rse-web.it

Diana MONETA
Ricerca sul Sistema Energetico – Italy
diana.moneta@rse-web.it

ABSTRACT

Extreme weather events may disrupt the transmission and distribution (T&D) network infrastructure, with consequent interruption of the power supply. Facing this issue requires in-depth analyses of the vulnerabilities of T&D components to natural threats, and deploying suitable measures to prevent the resulting - also multiple, dependent - contingencies. To this aim, the authors have developed a comprehensive methodology and tool, based on the risk concept, to assess the resilience of T&D networks as a whole. Simulations, performed on the model of a portion of the Italian T&D grid including two MV (Medium Voltage) feeders and a part of the surrounding transmission system in Aosta Valley, demonstrate the ability of the tool in identifying the critical components in presence of threats and in quantifying the resilience benefits brought by reinforcements (e.g. reconductoring) or operational solutions (e.g. reconfiguration of MV counterfeeds).

INTRODUCTION

The increasing frequency of extreme weather events, affecting both transmission and distribution networks, pushes Transmission System Operators (TSOs) and Distribution System Operators (DSOs) to evaluate the impact of multiple dependent outages of components, possibly leading to blackouts, and to propose preventive or corrective countermeasures to absorb the effects of such disruptive events and to recover fast, i.e. to increase system resilience [1][2]. In this context, current Italian regulation [3] imposes operators to publish and update a plan for resilience enhancement on a yearly basis.

The assessment of the effects of these extreme events on the grid and their mitigation call for an in-depth analysis on the vulnerabilities of T&D components to natural threats, as well as on the deployment of suitable measures to prevent the resulting -also multiple, dependent- contingencies.

The difficulty of the analysis is also due to the fact that distinct tools are generally used to perform decoupled analyses on T&D systems, even though mutual potential effects can take place in case of a contingency, e.g. the outage of High Voltage (HV) lines can cause the loss of supply of HV/Medium Voltage (MV) substations with potential loss of supply of the customers at distribution level. Reference [1] proposes a tool to evaluate the benefits to resilience brought by the deployment of grid hardening measures: they are typically focused on the transmission system and on one or few specific threats, with ad hoc models for threats and component vulnerabilities. In [4] the authors propose a methodology to study distribution network resilience to earthquakes under two particular strategies: one that hardens substations infrastructure in order to reduce their fragility levels, and the other one that uses additional network infrastructure in the form of transfer cables to shift load between substations in case a major event occurs.

The key and innovative feature of the proposed methodology is that it is "comprehensive" under two aspects: (1) it can model a wide set of natural threats (from wet snow to pollution, floods, etc.), (2) it can simulate the response of the integrated T&D system to disturbances, catching the potential mutual effects between MV and HV grids. Moreover, modeling different hardening and smart countermeasures allows to quantify their benefits to system resilience.

After an overview of the rationale, the paper presents the methodology and tool for resilience assessment. A case study is then presented, regarding two MV feeders connected to the surrounding HV grid in Aosta Valley. Simulation results demonstrate the modeling flexibility of the tool and its potential in supporting a resilience-oriented operation and planning of the overall grid.

METHODOLOGY AND TOOL

An extended risk based approach

The resilience assessment methodology applies the model illustrated in [5] to describe the connections between threats, component vulnerabilities, and power system contingencies. Natural and/or human-related threats may lead to a contingency through a set of causes exploiting vulnerabilities, while the contingency might lead to different impacts depending on the circumstances. The initial impact may in turn affect other vulnerabilities, starting a cascading process that may eventually result into a blackout. In order to quantitatively assess the relationship between root causes (threats) and power system disturbances (contingencies), the methodology extends the classical concept of risk [6] as a set of triple (contingency, probability, impact) and defines risk as a set of quadruple (threat, vulnerability, contingency, impact) where the *probability* term is replaced by the probabilistic models associated to threats and vulnerabilities. This means that the failure probability of each component in the time interval $\Delta t = t - t_0$ is expressed as a function of the average models $p_{Thr}^{(\Delta t)}(t_0, s, x)$ and $P_V^{(\Delta t)}(t_0, s, x)$ respectively representing

the spatial dependent probability density function (pdf) of the relevant stress variable S and the conditional probability function of failure over Δt for a component located in x, as reported in (1).

$$P_F(x,\Delta t,t_0)=\int_S P_V^{(\Delta t)}(t_0,s,x)\cdot p_{Thr}^{(\Delta t)}(t_0,s,x)ds \qquad (1)$$

This extended risk definition allows to link Probabilistic Hazard Assessment (PHA) studies to Security Assessment (SA) analyses, focusing on the root causes of disturbances. This step forward also allows to select the dangerous contingencies, to be simulated in detail, on the basis of current or expected environmental/weather conditions, thus complementing conventional security analyses based on the classical N-1 criterion.

Modeling threats and component vulnerabilities

The computation of the last term of (1) requires the knowledge of the dependence of the stress variable pdf at location x. The tool allows to characterize the threat geospatial models in two ways:

(1) in *operational planning mode*, where weather variable geospatial distributions come from a forecasting system available at the control center;
(2) in *engineering mode*, by analytical functions which characterize in probabilistic terms the intensity and extension of the threat.

In engineering mode, threats are modelled using either standard or customised geospatial distributions of the expected values for stress variables, as shown in Table 1.

Table 1: Stress variables for the analyzed threats

Threat	Stress variable [measurement unit]	Stress variable spatial distribution
Ice and snow	Wind+Ice load [N/mm^2] Conductivity on insulators [µS/cm^2]	customised
Pollution	Pollution concentration on insulators [mg/cm^2]	standard
Lightnings	Flash to ground density [# flashes/(km^2*h)]	standard
Earthquake	Peak ground acceleration [m/s^2]	customised
Physical attacks	Attack scenario probability [# attacks/week]	customised
Landslides	Newmark displacement [m]	customised
Floods	Water level [m]	standard
Fires	Insulation temperature [°C]	standard
Vegetation	Tree height [m]	standard
Thermal Ageing	Air temperature [°C]	standard

The standard spatial distributions consist in Gaussian-like functions (see [5]), while customized models depend more specifically on the physics of the modelled threats.
Each HV and MV component is characterized by a vulnerability function which is specific for each threat and can be derived from ad hoc tests, mathematical models, or qualitative information from experts.

The tool

Figure 1 shows the architecture of the tool for risk-based resilience assessment [5].
The tool combines the short term models of a hazard (*wet snow storm*, *lightning*, *fires*, etc.) with the vulnerability curves of the power system components, thus getting the failure probabilities of components over time horizons from few hours to few minutes ahead.

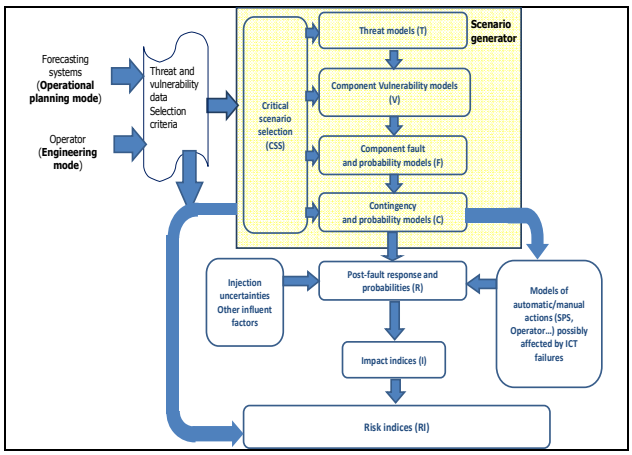

Figure 1: Architecture of the tool for risk-based resilience assessment

After that, the tool carries out the following tasks:

- select the critical components, defined as the ones which have the highest failure probabilities and contribute to a fraction δ of the sum of the failure probabilities over all the components;
- generate a comprehensive set of multiple, common mode and dependent contingencies involving the critical components;
- identify the most risky contingencies establishing a minimum risk threshold R_{min} by using a fast screening method, based on ex-ante topological risk indexes.

The retained contingencies are simulated using a quasi-static cascading outage simulator in order to evaluate the potential cascades triggered by the initiating events, thus computing indicators such as the amount of MW's lost or the energy not served. This cascading outage simulator is based on a robust power flow program enhanced with steady-state models of frequency regulation and of the main protection and defence systems. It also models the switching of normally open counterfeeds to restore loads in MV networks.
The risk-based resilience indicator in case of generic contingency j is given by (2).

$$Resilience_{ctg,j}=\frac{1}{Risk_{ctg,j}}=\frac{1}{\left(p_{ctg,j}\times Imp_{ctg,j}\right)} \qquad (2)$$

where $p_{ctg,j}$ is the probability of the contingency while impact indicator $Imp_{ctg,j}$ is given by the loss of load.

MODELING DISTRIBUTION NETWORKS RESILIENCE TO WET SNOW THREAT

This section discusses some modeling aspects related to wet snow events heavily affecting distribution networks.

Wet snow events

Under specific conditions of temperature (0°C-2°C), the snowflakes can partially melt and settle on the conductor and join together not only by the mechanism of collision, but also for the strong coalescence due to the presence of Liquid Water Content (LWC) in the snowflakes that promotes the growth of sleeve typically cylindrical in shape around the wire. The snow sleeves up to 15 cm in diameter can cause an extra load on conductors up to 8-10 kg/m, producing serious damages to overhead lines (OHLs). In some cases, the conductor undergoes an extra

load due to the intense wind blowing after the accretion event. The threat model [5] accounts for the wind speed and direction, the ambient temperature and the precipitation rate. The methodology [8] adopts the wet snow mass accretion model described by ISO [7].

The most vulnerable components to wet snow events are the OHLs with bare conductors in MV and HV/EHV grids, and the aerial cables in MV networks.

The vulnerability probabilistic models for OHLs with bare conductors includes the vulnerability of:

a) the phase conductors and the shielding wires which are affected by the mechanical tension due to the combined ice-wind load;
b) the tower equipment (insulator chains, and bracings) subject to combined force due to wind and ice loads.

As for item a), a mechanical fragility curve is evaluated for each phase conductor and shielding wire consisting in a lognormal distribution of mechanical tension with a mean value equal to the expected tensile strength in kN for the conductor (e.g. 170 kN for a 31.5 mm ACSR conductor used for phase conductors of HV lines) and a standard deviation equal to 2% of the expected value. The failure probability of individual line span is calculated by combining the failure probability related to the phase conductors, the shielding wires and the tower equipment.

In MV networks OHL lines with bare conductors usually don't have shielding wires. Instead, the pole of a MV line can be severely affected by wet snow, thus its vulnerability curve cannot be neglected. On the contrary, for HV and EHV lines, the mechanical failure of the towers is neglected because lattice towers are much less vulnerable to ice and wind loads with respect to tower equipment like the bracings. Moreover the most used configuration for MV aerial cable lines is characterized by three cables wrapped around a 9 mm diameter galvanized steel wire. The mechanical action on cable lines is essentially carried out on the supporting wire, whose vulnerability is given by a lognormal probability distribution with an expected value of 62 kN (for a 9 mm diameter steel wire) and a 2% standard deviation.

Countermeasure modeling

The measures to boost system resilience [9] in case of natural threats can be classified into two categories:

- passive approaches, aimed at improving the ability of the infrastructure to not be damaged in case of threats, by preventing and minimizing their impact via the introduction of redundancies, the hardening of the components, and the use of protective barriers;
- active approaches, aimed to minimize disruptions, to improve system absorption capability, recovery speed.

Two examples of passive and active measures are respectively the reconductoring, i.e. the upgrade of the mechanical strength of conductors by adopting larger diameters for the conductors, and the optimal reconfiguration of counterfeeds.

Reconductoring can be applied both to the HV and to the MV grids, given that in some cases a potential upgrade of the physical supporting infrastructure (i.e. the towers/poles) must be performed in order to withstand the increased weight of the new conductors.

The process of reconfiguring counterfeeds following a contingency that determines the out-of-service of network components (for example MV connections, or secondary or primary substations) can have different objectives:

- maximize the load restored to users (main goal);
- minimize the number of maneuvers;
- reduce active losses in the post-contingency network configuration.

The reconfiguration optimizer adopted in the tool exploits the modified Viterbi algorithm [10].

CASE STUDY

This section presents a case study referring to threat "wet snow", describes the grid model, the threat scenarios and discusses the simulation results obtained from the risk based resilience assessment tool.

Grid model

The test system under study integrates two MV feeders, Smart Grid" Deval project promoted by ARERA [11], with a portion of the surrounding HV/EHV transmission grid in Aosta Valley, specifically around HV/MV primary substation at Villeneuve, particularly critical in terms of operation and maintenance as it provides energy to a very large area (about 770 km^2).

Figure 2 provides an overview of the integrated MV and HV grid under study. The dashed lines in Figure 2a) are MV feeders excluded from the present analysis.

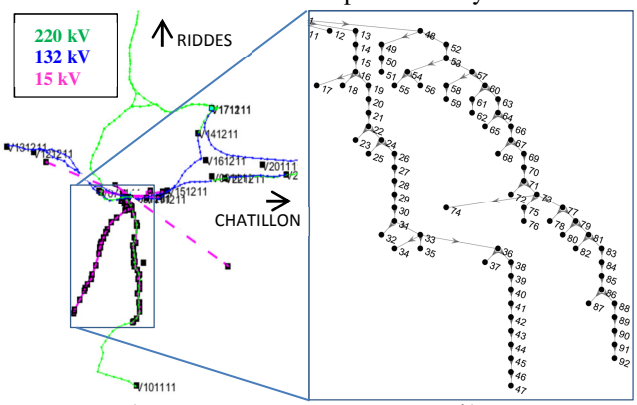

a) b)

Figure 2: The integrated MV/HV/EHV grid: (a) map of the MV feeders and of surrounding HV grid, (b) the one-line diagram of the two feeders

The resulting MV/HV grid model is derived from Aosta Valley map [12], Deval [11], as well as ENEL and TERNA standards [13][14], and it includes 92 MV electrical nodes, of which 60 nodes are MV/LV substations, 29 transit nodes in correspondence of line poles, and 3 the HV and MV busbars at Villeneuve HV/MV substations. Three main counterfeeds can connect the following nodes: Champagne – Thumel Caverna (#12 - #46); Bouillet – Camping (#26 - #31); Bouillet-Dir. Bouillet (#26 - #63). The rated transformation power at MV/LV substations is estimated on the basis of the size of the population served by each MV/LV substation: 50, 100, 160 and 250 kVA. The model also includes 10 HV (132 kV) nodes, 8 EHV (220 kV) nodes as well as 20 OHLs, 6 generators and 3 EHV/HV transformers.

It's worth noting that a unique model is used in the platform to represent the overall system; the hazard analysis and the simulation of the system response to the disturbances are performed only once on the same integrated grid model.

Simulation scenarios

Table 2 reports the main features of the wet snow storm scenarios adopted in the simulations.

Table 2: Expected values for parameters characterizing wet snow events

Hazard parameter	S1 (moderate)	S2 (severe)
Peak wind speeds	10-15 m/s	10-15 m/s
Precipitation rate	1 mm/h	5 mm/h
Initial precipitation level	10 mm	20 mm
air temperature	-0.5°C -1.5°C	-0.5°C -1.5°C

The following simulation cases are discussed in the paper: the wet snow storm base cases S1 and S2, the application of reconductoring in scenario S1, the construction of a new counterfeed and the application of optimal reconfiguration algorithm in scenario S2.
For all the simulations the following parameters for the wet snow events are assumed as fixed parameters:

- diameter of the wet snow precipitation area = 80 km;
- diameter of the wind swept area = 35 km;
- threat center around Villeneuve substation.

Unless differently specified, the fraction of explained total failure probability is set to 0.95. Moreover, all the components with a failure probability higher than (or equal to) 10% are considered as critical components.

S1 base case

For all the overhead conductors in MV and HV grids Figure 3 reports the expected values of the stress variables (i.e. the mechanical tension) on the conductors, and the loads due to wet snow and wind.

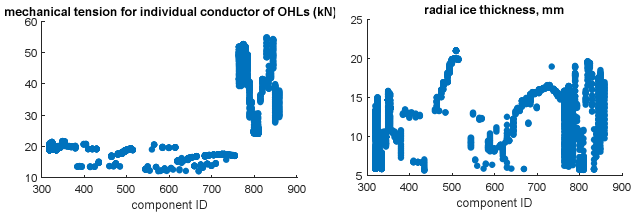

(a) (b)

Figure 3: Mechanical tension (a) in kN, and wet snow sleeve thickness (b) for MV and HV lines, scenario S1 moderate wet snow

In Figure 4 the critical components (in particular, branches) are represented using a specific color to represent their conditional probability of failure (white for probabilities lower than 0.2, cyan for probabilities between 0.2 and 0.4, yellow for probabilities between 0.4 and 0.6, red for probabilities between 0.6 and 0.8, magenta for probabilities higher than 0.8).

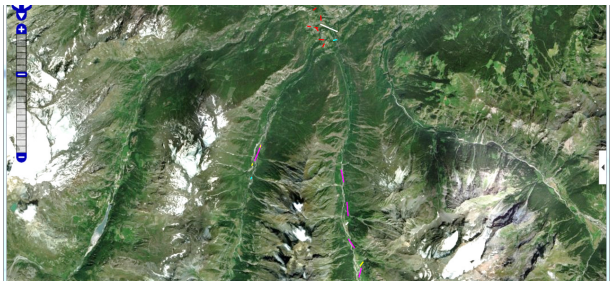

Figure 4: Geolocalization of critical components, scenario S1 moderate wet snow storm

Figure 5 reports the contributions (in terms of expected lost MW) of each contingency category to the total risk of loss of load. The largest contributions to the total risk are associated to high order common mode branch outages (N-13 and N-14): in fact most of the selected critical lines have a very high probability of failure.

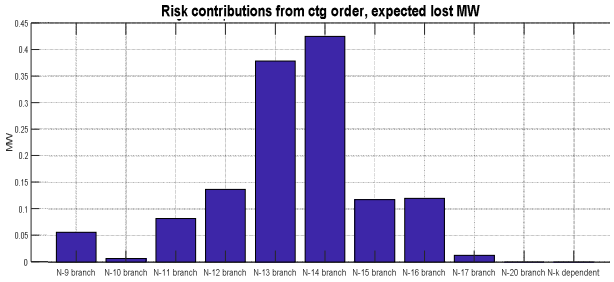

Figure 5: Contributions to total risk of each contingency category, scenario S1

Effect of reconductoring

The critical OHLs with a 35 mm^2 section undergo an upgrading process which changes the section areas from 35 mm^2 to 70 mm^2. This decreases noticeably the failure probability of critical components (the highest failure probability becomes 7.15×10^{-1}). The total risk of loss of load over 10 minutes passes from 1.33 expected lost MW in S1 to 0.72 expected lost MW in the present case.

Effect of a new counterfeed on S2 scenario

The application of the severe wet snow event S2 to Villeneuve area determines a set of 52 critical branches, of which 37 have a failure probability higher than 90% and 15 a failure probability between 0.9 and 0.1.
The high severity of S2 event determines a very high probability of damage not only on small section branches (35mm^2) section but also on main branches of the two feeders (such as 40-41) with higher sections (70 mm^2). The risk of losing a very large set of branches (up to 52) is much higher than in moderate wet snow scenario S1.
To counteract such criticality, a new counterfeed is supposed to be built between node 48 (Dir Crete de Ville) and node 91 (Pont), chosen because no counterfeeds can assure to restore the 100% of total lost load in case of a fault on main branches around nodes of range [70-90].
The same simulation of S2 event is performed assuming that only a single counterfeed is activated for each contingency, which is in line with the usual operating practice. The application of the new counterfeed does not change much the average value of the LOL risk indicators over the whole set of contingencies (undergoing a 1% decrease) but significantly reduces the impact for a set of about 20 contingencies. Figure 6 compares the LOL impact of these contingencies before and after the introduction of the new counterfeed.

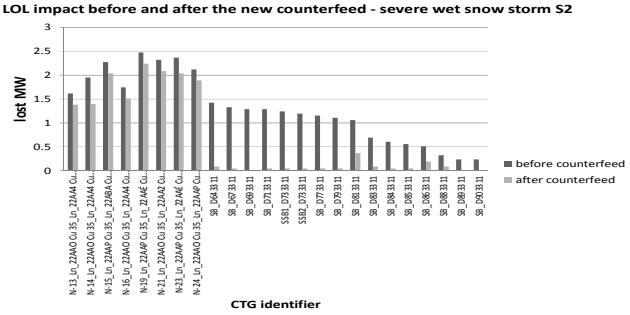

Figure 6: Bar diagram of the LOL impact of the contingencies before and after the new counterfeed, severe wet snow event S2

The largest reduction of loss of load is detected for the busbar contingencies affecting nodes 64 thru 90 along the feeder in Valsavaranche valley which contains also the terminals of the counterfeed i.e. nodes 48 and 91. On the contrary, N-51 and N-52 contingencies provoke so large disruptions that the activation of a single counterfeed cannot reduce the loss of load caused by the contingency.

Optimal reconfiguration of counterfeeds

This case considers the N-2 outage of two critical branches 40-41 and 16-19 in S2 base case (see Figure 2) which determines the loss of supply of many customers connected to the Rhemes Valley feeder.
Table 3 reports the main indicators, i.e. the minimum MV voltage M_V, the percentage of restored load and the active power losses *plosses* obtained after the application of any one or two switching reconfigurations. In this case there is no "one switching" reconfiguration of a counterfeed (k=1) which allows to restore all the unsupplied load.

Table 3: Performance indicators for different manoeuvres on counterfeeds, outage of branches 40-41 and 16-19

state	M_V	Percentage of restored load (%)	*plosses*, MW
001	0.9951	66.67	0.0119
010	0.9987	48.30	0.0087
100	0.997	81.63	0.0125
011	0.9951	66.67	0.0119
101	0.9951	100	0.0156
110	0.9975	81.63	0.0109

Thus, the optimal reconfiguration algorithm checks all the reconfigurations of two counterfeeds (k=2). Only one reconfiguration with k=2, i.e. $X_{63\text{-}26}$=1 , $X_{26\text{-}31}$=0 e $X_{12\text{-}46}$=1, allows to restore all the unsupplied load with a minimum number of maneuvers, while keeping also the radiality of the post-contingency network topology.

CONCLUSIONS

This paper has presented an innovative tool for risk based assessment of the resilience of MV/HV systems subject to threats. Simulations, performed on a detailed model of a real-world MV grid (i.e. two MV feeders in the Deval network in Aosta Valley) integrated with the surrounding HV/EHV grid, have demonstrated the main capabilities of the tool, i.e. its ability to simulate the response of the MV/HV grid and its flexibility to model the detailed vulnerability curves for the grid components of both MV and HV grids, as well as to quantify the benefits of some resilience boosting measures (reconductoring and reconfiguration of counterfeeds), in terms of reduction of loss of load risk, in case of threats with different severities. Though the described example focuses on wet snow events, the methodology can simulate a wide set of natural threats thanks to its general modeling framework, and it may represent a useful tool for resilience oriented planning and operational planning.
Future works concern the characterization of other threats (e.g. tree contact, lightnings, etc.) for the Deval system in view of further applications of the proposed tool.

Acknowledgments

This work has been financed by the Research Fund for the Italian Electrical System in compliance with the Decree of Minister of Economic Development April 16, 2018. The authors gratefully acknowledge also the contributions of Deval Operational division.

REFERENCES

[1] M. Panteli and P. Mancarella, 2015, "Influence of extreme weather and climate change on the resilience of power systems: impacts and possible mitigation strategies," *El. Power Systems Research*, pp. 259-270.

[2] ACER (Agency for the Cooperation of Energy Regulators), 2014, "European Energy Regulation: A bridge to 2025", report.

[3] ARERA (Italian Regulatory Authority for Energy, Networks and Environment), 2017, "Determina 2/2017 - Linee guida per la presentazione dei Piani di lavoro per l'incremento della resilienza del sistema elettrico", deliberation (in Italian).

[4] A. Navarro-Espinosa et al., "Improving distribution network resilience against earthquakes," *Proc. of IET Int. Conf. on Resilience of Transmission and Distribution Networks (RTDN 2017)*, Birmingham, 2017, pp. 1-6.

[5] E. Ciapessoni, D. Cirio, G. KjØlle, S. Massucco, A. Pitto and M. Sforna, 2016, "Probabilistic risk based security assessment of power systems considering incumbent threats and uncertainties," Special issue on "Power System Resilience" *IEEE Trans. on Smart Grid*, vol. 7, no. 6, pp.2890-2903.

[6] M. Ni, J. D. McCalley, V. Vittal and T. Tayyib, 2003, "Online Risk-Based Security Assessment," *IEEE Trans. on PS*, vol. 18, no. 1, pp. 258-265.

[7] ISO Std. 12494, 2017, *Atmospheric icing of Structures*.

[8] P. Admirat and Y. Sakamoto, 1988, "Calibration of a wet-snow model on real cases in Japan and France," *Proceedings of 4th Int. Workshop on Atmospheric Icing of Structures*, vol. 1.

[9] M. Farzaneh, C. Volat and A. Leblond, 2008, *Anti-icing and de-icing techniques for overhead lines* in *Atmospheric icing of power networks*, Springer, Dordrecht.

[10] C. Yuan, M. S. Illindala and A. S. Khalsa, 2017, "Modified Viterbi Algorithm Based Distribution System Restoration Strategy for Grid Resiliency," *IEEE Trans. on Power Delivery*, vol. 32, no. 1.

[11] Deval, 2015, "Progetto Smart Grid - Cabina Primaria di Villeneuve", final report (in Italian).

[12] Regione Val d'Aosta, 2018, "Geographic Information System (GIS),". Available: http://geonavsct.partout.it/pub/GEoCartoSCT/.

[13] e-Distribuzione, 2008, "Modalità e Condizioni Contrattuali per l'erogazione da parte di Enel Distribuzione del Servizio di Connessione alla Rete Elettrica con Tensione Nominale Superiore ad 1 kV," report (in Italian).

[14] A. Guarneri and M. Forteleoni, 2011, "Caratteristiche generali delle linee elettriche aeree facenti parte della RTN", TERNA report (in Italian).